Bond behavior between glulam and GFRP's using pullout bending tests

Marco Jorge
MSc, Technician, Dep. of Civil Engrg.
Univ. of Minho (Guimarães)
marco@civil.uminho.pt

José Sena-Cruz
PhD, Assistant Professor, Dep. of Civil Engrg.
Univ. of Minho (Guimarães)
jsena@civil.uminho.pt

Jorge Branco
PhD, Assistant Professor, Dep. of Civil Engrg.
Univ. of Minho (Guimarães)
jbranco@civil.uminho.pt

Joaquim Barros
PhD, Associate Professor, Dep. of Civil Engrg.
Univ. of Minho (Guimarães)
barros@civil.uminho.pt

Gláucia Dalfré
PhD student, Dep. of Civil Engrg.
Univ. of Minho (Guimarães)
gmdalfre@civil.uminho.pt

Palavras-chave – Glulam; varões de polímeros reforçados com fibras de vidro; técnica NSM; ensaios de arrancamento por flexão

Keywords – Glulam; GFRP rods; NSM strengthening technique; pullout bending tests

RESUMO

Com o objectivo de avaliar o comportamento da ligação entre lamelados colados e varões de GFRP, quando aplicados de acordo com a técnica NSM, foi realizado um programa experimental composto por ensaios de arrancamento por flexão. Neste programa experimental foram analisadas três variáveis: o tipo de GFRP (2 tipos), a localização do FRP/dimensão da ranhura (2 tipos) e o comprimento de amarração (L_b=30 mm, 60 mm, 120 mm e 180 mm). A instrumentação inclui a medição dos deslizamentos na zona solicitada e na extremidade livre, bem como a força de arranque. Vinte e nove provetes foram ensaiados sob controlo de deslocamento com recurso a um sistema servo-controlado. O presente trabalho descreve os ensaios e apresenta e discute os resultados obtidos.

ABSTRACT

To evaluate the bond behavior between glulam and GFRP rods using the near-surface mounted (NSM) strengthening technique, an experimental program was carried out by means of pullout bending tests. In this experimental program three variables were analyzed: the GFRP type (2

types), the GFRP location/groove size (2 types) and the bond length (L_b=30 mm, 60 mm, 120 mm and 180 mm). The instrumentation includes the loaded and free end slips, as well as the pullout force. Twenty nine specimens were tested under displacement control using a servo controlled equipment. In this work the tests are described, and the obtained results are presented and discussed.

1. Introduction

The origin of glued laminated (glulam) timbers occurred in the beginning of the XX century, by Otto Hetzer. Since then, glued laminated technology faced great improvements. Nowadays, the manufacturing process of glulam is strict and industrialized, which makes the geometry very precise, controlled moisture content and mechanical properties with less dispersion. This leads to a higher mechanical resistance and elasticity modulus when comparing to solid wood. Glulam materials have widely been used in transportation infrastructures (e.g. bridges), and in roofs of pavilions.

In the last decades fiber reinforced polymer (FRP) materials have been tested and used to repair or strengthen existing structures. High stiffness and tensile strength, low weight, easy installation procedures, high durability (no corrosion), electromagnetic permeability and practically unlimited availability in terms of geometry and size are the main advantages of these composites (ACI 2008).

Currently, the most used strengthening techniques using FRP systems are (ACI 2008, Bank 2004): the externally bonded reinforcement (EBR), the near-surface mounted (NSM) technique, and the mechanically fastened FRP (MF-FRP). In the context of any strengthening technique, bond behavior is an important issue, since it governs the performance of the composite strengthening system. The bond performance influences not only the ultimate load-carrying capacity of a reinforced element but also some serviceability aspects, such as deformation and crack width. In the last decades several test methods have been proposed and used in the bond research, mainly in concrete material. The most common are the direct and the beam pullout tests. At the present time, there is no general agreement about the correct test setup to assess the bond behavior for the distinct FRP systems (Barros and Costa 2010).

In order to study the bond behavior between glulam and GFRP rods with the near-surface mounted (NSM) strengthening technique, an experimental program through pullout bending tests was carried out. The influence of GFRP type, the groove geometry/FRP location and the bond length, on the bond behavior was studied. In the following sections tests are described in detail, and the obtained results are discussed.

2. Experimental Program

2.1. Specimens and Test Configuration

The experimental program was composed by twenty nine pullout bending tests, grouped in series of two, three or four specimens. Bond lengths ranging between 30 and 180 mm were adopted in order to assess its influence on the bond behavior.

The code names given to the test series consist on alphanumeric characters separated by underscores (see Table 1). The first string indicates the GFRP type (GFRP1 and GFRP2). The second string defines the depth at which the FRP was installed into the groove (D1 and D2). Finally, the last string indicates the bond length in millimeters (for instance, Lb30 represents a specimen with a bond length of 30 mm).

Fig. 1 shows the specimen geometry and the pullout bending test configuration of all the series tested. The specimen is composed by two glulam blocks (block A and B) of equal dimensions, $140 \times 200 \times 300$ mm^3, interconnected by a steel hinge located at mid-span in the top part, and also by the FRP fixed at the bottom in which the FRP is embedded. The bond test region was located in the bottom part of block A, and several bond lengths, L_b, were analyzed (see Table 1). To avoid premature splitting failure in the glulam ahead the loaded end (Sena-Cruz *et al.*, 2001), the bond length started 50 mm far from the block end.

The instrumentation of the specimens consisted on two linear variable differential transducers (LVDT), a strain gauge and a load cell. The displacement transducer LVDT2 was used to control the test, at 2 μm/s slip rate, and to measure the slip at the loaded end, s_l, while the LVDT1 was used to measure the slip at the free end, s_f. The applied force, F, was transmitted to the specimen through a steel plate that, in turn, transmits $F/2$ through two steel rods to the glulam blocks. The applied force was registered by a load cell placed between the steel plate and the actuator.

Material	**Depth** (mm)	L_b (mm)	**Denomination**	**Number of specimens**
GFRP1	20	30	GFRP1_D2_Lb30	3
		60	GFRP1_D2_Lb60	3
		120	GFRP1_D2_Lb120	3
		180	GFRP1_D2_Lb180	2
	15	30	GFRP1_D1_Lb30	4
		60	GFRP1_D1_Lb60	2
		120	GFRP1_D1_Lb120	4
GFRP2	15	30	GFRP2_D1_Lb30	2
		60	GFRP2_D1_Lb60	4
		120	GFRP2_D1_Lb120	2

Table 1 – Experimental program

To evaluate the pullout force applied to the GFRP rod at the loaded end section, a strain gauge was bonded on the FRP rod at the specimen middle span (see Fig. 1).

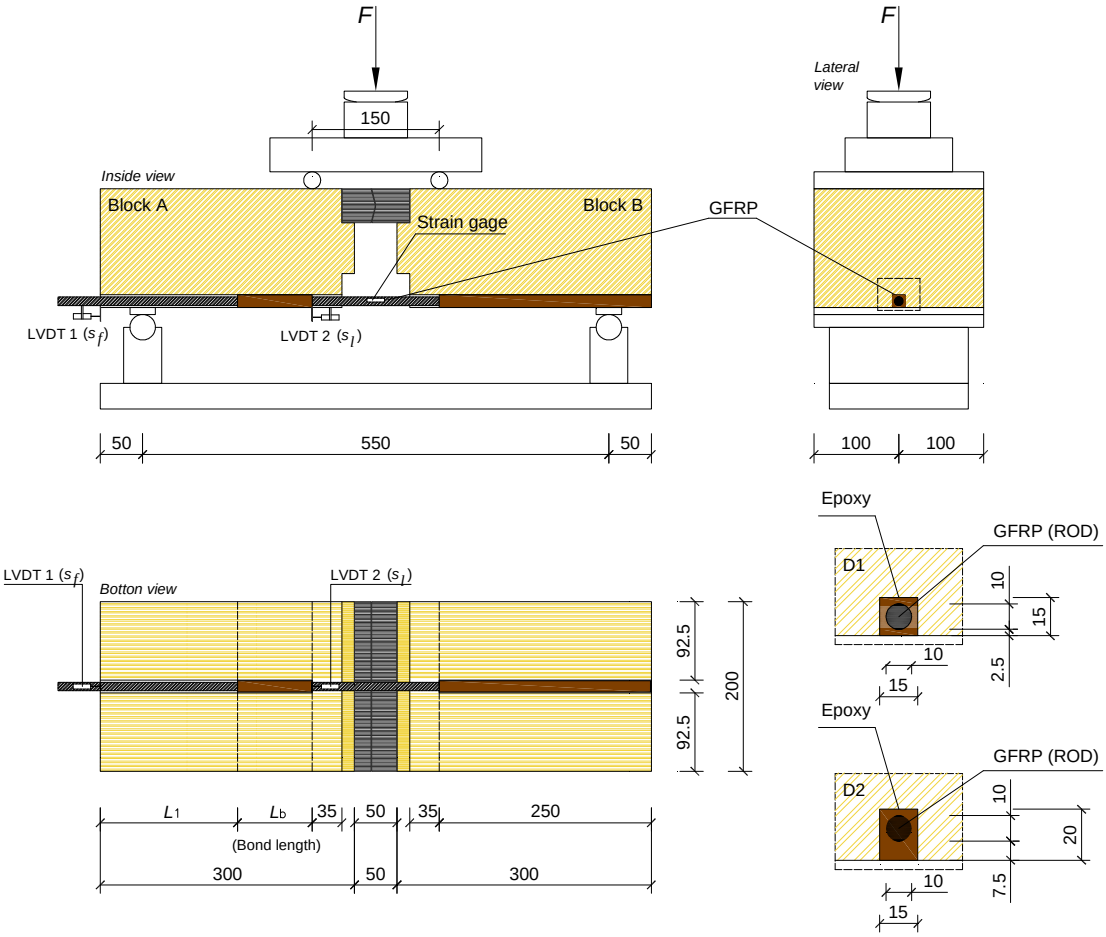

Figure 1 – Specimen geometry and pullout bending test configuration. Note: all dimensions are in [mm].

2.2. Material characterization

2.2.1. Timber

In the present experimental program glulam timber of strength class GL24h (NP EN 1194:1999) was used for all the series. The material characterization of the GL24h included compression and tension parallel to the grain tests according to EN 408 (CEN 2003).

From the compression tests an average compressive strength of 27.99 MPa with a coefficient of variation (CoV) of 17.6%, and an average modulus of elasticity of 6.62 GPa (CoV=27.8%) were obtained. Additional details can be found elsewhere (Jorge, 2010).

From the tension tests, an average tensile strength, modulus of elasticity and strain at the peak stress of 55.93 MPa (CoV=16.7%), 9.17 GPa (CoV=11.9%) and 6.35‰ (CoV=12.4%) were obtained. Further details can be found elsewhere (Jorge 2010).

2.2.2. GFRP rod

The GFRP rod used in the present work, with a trademark Maperod G, was provided in rolls of 6 meters each, and was supplied by MAPEI®. Two distinct types of Maperod G were used with different external surface (see Fig. 2). Herein, the rod with a rougher external surface was denominated as GFRP2, whereas the other as GFRP1. These rods have a diameter of 10 mm and the external surface is sand blasted.

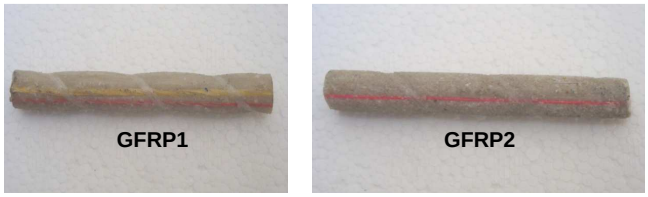

Figure 2 – GFRP used in the experimental program

Tension tests were carried out to assess the tensile mechanical properties of each GFRP rod type, according to ISO TC 71/SC 6 N - Part 1 - (2003).Tests were performed under a displacement rate of 2 mm/min. To measure the modulus of elasticity, a clip gauge was mounted at middle region of each specimen. The results obtained from the mechanical characterization of the GFRP rods are presented in Table 2. Both GFRP rods have similar response, not only in terms of tensile strength but also in terms of modulus of elasticity. However, GFRP2 presents a modulus of elasticity slightly higher. Very low values of the coefficients of variation (CoV) were obtained for the case of GFRP1, but a rather high value of CoV was registered for the strain at the maximum tensile stress for the GFRP2.

GFRP	F_{fmax} (kN)	σ_{fmax} (MPa)	E_f (GPa)	ε_{fmax} (‰)	***Failure mode***
GFRP1	61.12 (3.5%)	778.14 (3.5%)	38.42 (1.3%)	20.25 (2.3%)	XGM (all)
GFRP2	61.15 (1.6%)	786.04 (2.8%)	41.60 (7.8%)	18.99 (10.2%)	OGM (all)

Notes: F_{fmax}= maximum force; $\sigma=F/(\pi\times10^2/4\ mm^2)$; σ_{fmax}= tensile strength; E_f = longitudinal elasticity modulus; ε_{fmax}= strain at σ_{fmax}; $\varepsilon_{fmax}=\sigma_{fmax}$ / E_f; E_f is the slope of curve σ–ε between 20% and 50% of σ. Failure modes: XGM – Explosive failure in gage measuring length; OGM – Failure occurred outside the clip gauge measuring region. The values between parentheses are the corresponding coefficients of variation.

Table 2 – Main results obtained on the mechanical characterization of the GFRP rods (average values)

2.2.3. Epoxy adhesive

In the present experimental work the epoxy MapeWood Paste 140, supplied by MAPEI®, was used. This thixotropic epoxy adhesive is currently used for the restoration of timber structural elements, and is composed of two premeasured parts (Part A = resin and Part B = hardener).

To assess the mechanical properties of each hardened adhesives, tensile tests were carried out according to ISO 527-2 (1993). After casted, the specimens were kept in the laboratory environment, and when tested they had the same age of the adhesive of the pullout tests. The adhesive specimens were tested in a universal test machine, at a displacement rate of 1 mm/min. A clip gauge mounted on the middle zone of the specimen recorded the strains and a high accuracy cell load has registered the applied force. Table 3 includes the main obtained results. A relatively large coefficient of variation for E_f e ε_{fmax} was obtained.

Adhesive	$F_{adh,max}$ (kN)	$\sigma_{adh,max}$ (MPa)	E_{adh} (GPa)	$\varepsilon_{adh,max}$ (‰)	***Failure mode***
MapeWood Paste 140	0.69 (8.4%)	17.15 (7.5%)	8.11 (17.6%)	2.60 (19.6%)	OR (3) + IR (3)

Notes: $F_{adh,max}$= maximum force; $\sigma_{adh,max}$= uniaxial tensile strength; E_{adh}= longitudinal elasticity modulus; $\varepsilon_{adh,max}$= strain at σ_{fmax}; E_{adh} is the slope of the curve σ–ε between 0.0025 and 0.0075 of ε. Failure modes: IR - inside the clip gauge region; OR - outside the clip gauge region; GR grip region. The values between parentheses are the corresponding coefficients of variation.

Table 3 – Main results obtained on the mechanical characterization of the adhesive (average values)

2.3. Preparation of specimens

The glulam blocks used for the NSM pullout bending tests were supplied with the correct dimensions including the groove's geometry. For the series D1 the grooves had a width and a depth of about 15 mm, while for the case of D2 series the width and the depth was 15 mm and 20 mm, respectively.

Some details of glulam and FRP's preparations before the strengthening are shown in Fig. 3. These procedures include the following main steps:

i. A sanding wood was used to eliminate the wood chips inside the grooves formed during the sawing process;
ii. Then grooves were cleaned using compressed air;
iii. A masking procedure in the vicinity of the bonding areas was adopted to keep original aesthetic of the glulam surface after strengthening;
iv. A small tab, built with FRP material, was fixed at the loaded end to measure the loaded end slip;
v. Small latex delimiter pieces were made to assure the correct location of the FRP in the groove cross-section;
vi. To guarantee the desired bond lengths, pieces of plastic were glued on FRP's surfaces;
vii. The glulam blocks and FRP were cleaned with acetone to remove any possible dirt;
viii. The blocks were temporary connected with four wood sticks to keep the necessary space between them to insert the steel hinge before test.

The rods were fixed to the glulam grooves using the MapeWood Paste 140 epoxy adhesive. Fig. 3 also shows the main steps required to strengthen the glulam specimens. Preparation of the epoxy adhesive was performed according to the recommendations of the supplier. The grooves were filled with the epoxy adhesive using a spatula, and GFRP rods are cover with a thin layer of epoxy adhesive. Then, the FRP's were gradually inserted into the grooves and slightly pressed to force the epoxy adhesive to flow between the FRP and the groove sides. Finally, the epoxy adhesive in excess was removed and the surface was leveled.

The specimens were kept in the laboratory environment before being tested. The pullout tests were carried out at least 10 days after the application of the FRP reinforcement.

3. Results and discussion

The analysis is focused in the following results: maximum force, free and loaded end slips at the peak load, average bond stress at rod/adhesive and adhesive/glulam interfaces, and failure modes. In addition, the relationship between the pullout force and the loaded end slip is also analyzed. As already mentioned, the two types of GFRP rods used had similar mechanical properties, but GFRP2 had rougher external surface.

Figs. 4 to 6 show the average pullout force *versus* loaded end slip ($F_l - s_l$) relationships for the series GFRP1_D1, GFRP2_D1 and GFRP1_D2, respectively. This relationship is composed of a short linear branch followed by a nonlinear response up to peak load, and then a softening behavior with an appreciable residual pullout resistance. The nonlinear branch in the pre-peak phase is as pronounced as higher is the pullout force. From these figures is also visible that the peak pullout force and the slip at this load level increase with the bond length. Furthermore, comparing Fig. 4 and 5 it can be concluded that the rougher surface of the GFRP2 rod contributed to increase the peak pullout force and the corresponding loaded end slip (see also Tables 4 to 6). Fig. 4 and 6 show that the benefits in terms of peak pullout force derived from installing the GFRP bar into the groove as deeper as possible was only relevant for the larger bond length.

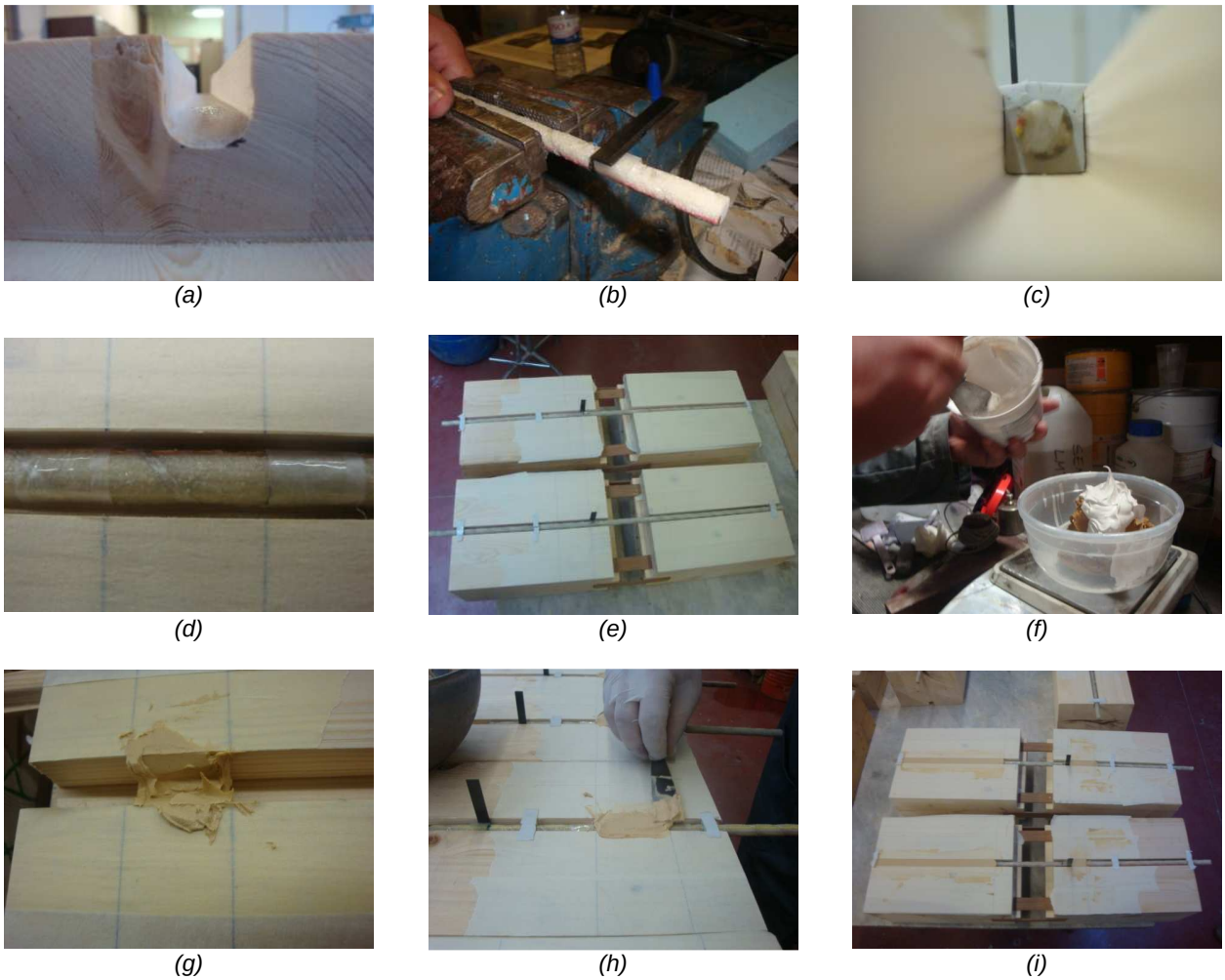

Figure 3 – Details of preparation of the specimens: (a) detail of the groove after liming; (b) FRP tab to measure the loaded end slip; (c) latex delimiters; (d) final state of the bond zone; (e) final state of the materials before the application of the strengthening; (f) epoxy adhesive preparation; (g) groove with epoxy adhesive; (h) leveling the surface; (h) final state of the specimens before removing the mask

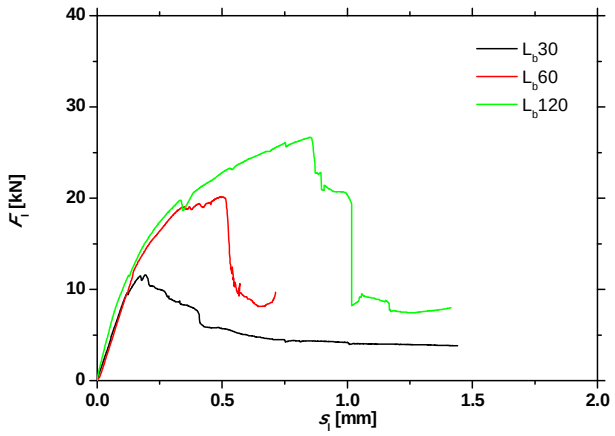

Figure 4 – Pullout force vs. loaded end slip for the series GFRP1_D1 (average curves)

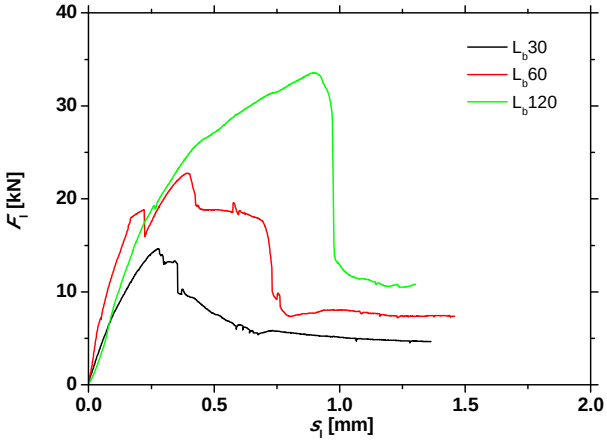

Figure 5 – Pullout force vs. loaded end slip for the series GFRP2_D1 (average curves)

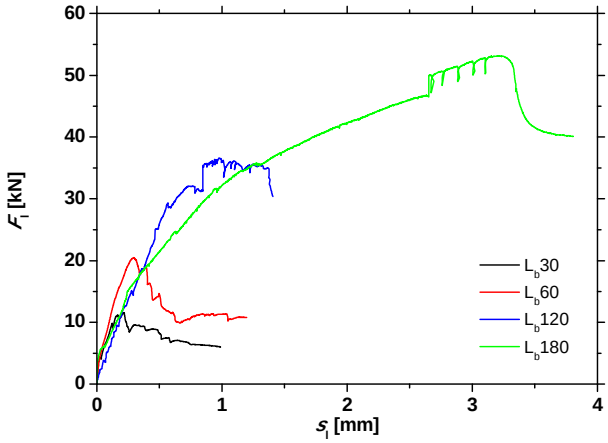

Figure 6 – Pullout force vs. loaded end slip for the series GFRP1_D2 (average curves)

Tables 4, 5 and 6 present the main results obtained for the series GFRP1_D1, GFRP1_D2 and GFRP2_D1, respectively. The pullout efficiency, defined by the F_{fmax} / F_{fu} ratio, was approximately equal to 87% for the GFRP1_D2_Lb180-3 (second specimen of the GFRP1_D2 series with a bond length of 180 mm). As expected, when the bond length increases, the maximum pullout force, F_{fmax}, increases and the average bond strength decreases (see columns of $\tau_{max,av1}$ and $\tau_{max,av2}$). However, these values are still quite high.

In general, all the parameters present quite low values of the corresponding coefficients of variation. The exception is for the values of slips at the loaded and free ends. In fact high coefficients of variation were observed, and main reason for that can be attributed to the difficulty in measuring this physical quantity.

Specimen	F_{fmax} (kN)	F_{fmax} / F_{fu} (%)	$\tau_{max,av1}$ (MPa)	$\tau_{max,av2}$ (MPa)	s_{fmax} (mm)	s_{lmax} (mm)	***Failure mode***
GFRP1_D1_Lb30-1	13.16	21.53	13.96	9.65	0.135	0.233	FAI+CR
GFRP1_D1_Lb30-2	11.14	18.24	11.83	8.06	0.001	0.187	FAI+CR
GFRP1_D1_Lb30-3	12.22	19.99	12.96	9.01	0.134	0.260	GAI+FAI+CR
GFRP1_D1_Lb30-4	10.71	17.53	11.37	7.78	0.081	0.119	FAI+CR
GFRP1_D1_Lb30	**11.81 (9.3%)**	**19.32 (9.3%)**	**12.53 (9.3%)**	**8.62 (10.0%)**	**0.09 (71.6%)**	**0.20 (31.0%)**	-
GFRP1_D1_Lb60-1	20.22	33.08	10.73	7.47	0.040	0.405	FAI+CR
GFRP1_D1_Lb60-2	20.16	32.99	10.70	7.39	0.199	0.494	FAI+CR
GFRP1_D1_Lb60	**20.19 (0.2%)**	**33.04 (0.2%)**	**10.71 (0.2%)**	**7.43 (0.7%)**	**0.12 (93.8%)**	**0.45 (13.9%)**	-
GFRP1_D1_Lb120-1	27.49	44.98	7.29	5.10	0.020	0.752	FAI+CR
GFRP1_D1_Lb120-2	27.78	45.46	7.37	5.03	0.034	0.983	FAI+CR
GFRP1_D1_Lb120-3	26.63	43.58	7.06	4.86	0.138	0.896	FAI+CR
GFRP1_D1_Lb120-4	27.78	45.46	7.52	5.03	0.034	0.983	FAI+CR
GFRP1_D1_Lb120	**27.42 (2.0%)**	**44.87 (2.0%)**	**7.31 (2.6%)**	**5.00 (2.1%)**	**0.06 (96.6%)**	**0.90 (12.1%)**	-

Notes: F_{fmax}= maximum pullout force; F_{fu}= FRP strength force; $\tau_{max,av1}$= average bond stress at the bar-epoxy interface at F_{fmax}; $\tau_{max,av2}$= average bond stress at the glulam-epoxy interface at F_{fmax}; s_{fmax}= free end slip at F_{fmax}; s_{lmax}= loaded end slip at F_{fmax}; FAI – interfacial failure FRP/adhesive; GAI – interfacial failure glulam/adhesive; SPL – adhesive splitting; GS – glulam shear failure; CR – adhesive cracking; FF – FRP failure.

Table 4 – Main results obtained in the series GFRP1_D1

Specimen	F_{fmax} (kN)	F_{fmax} / F_{fu} (%)	$\tau_{max,av1}$ (MPa)	$\tau_{max,av2}$ (MPa)	s_{fmax} (mm)	s_{lmax} (mm)	*Failure mode*
GFRP1_D2_Lb30-1	11.83	19.36	12.55	7.08	0.103	0.165	GAI
GFRP1_D2_Lb30-2	14.24	23.30	15.11	8.59	0.201	0.215	FAI+CR
GFRP1_D2_Lb30-3	11.85	19.39	12.58	7.07	0.088	0.121	FAI+GAI+CR
GFRP1_D2_Lb30	**12.64 (11.0%)**	**20.68 (11.0%)**	**13.41 (11.0%)**	**7.58 (11.5%)**	**0.07 (62.1%)**	**0.17 (28.2%)**	-
GFRP1_D2_Lb60-1	23.43	38.35	12.43	7.04	0.130	0.428	GAI
GFRP1_D2_Lb60-2	21.00	34.37	11.14	6.32	0.078	0.279	FAI+CR
GFRP1_D2_Lb60-3	22.94	37.54	12.17	6.90	0.114	0.383	G
GFRP1_D2_Lb60	**22.46 (5.7%)**	**36.76 (5.7%)**	**11.92 (5.7%)**	**6.76 (5.6%)**	**0.11 (25.3%)**	**0.36 (21.0%)**	-
GFRP1_D2_Lb120-1	33.77	56.29	8.96	5.03	0.095	0.968	GAI+FAI+CR
GFRP1_D2_Lb120-2	31.52	52.52	8.36	4.75	0.036	0.912	FAI+CR
GFRP1_D2_Lb120-3	37.57	62.62	9.97	5.67	0.054	0.966	FAI+CR
GFRP1_D2_Lb120	**34.29 (8.9%)**	**57.15 (8.9%)**	**9.10 (8.9%)**	**5.15 (9.1%)**	**0.06 (48.8%)**	**0.95 (3.4%)**	-
GFRP1_D2_Lb180-1	43.85	71.76	7.76	4.36	0.14	2.61	GAI+FAI+CR
GFRP1_D2_Lb180-3	53.13	86.95	9.40	5.29	0.24	3.22	GAI+G
GFRP1_D2_Lb180	**48.49 (13.5%)**	**79.36 (13.5%)**	**8.58 (13.5%)**	**4.83 (13.7%)**	**0.19 (35.7%)**	**2.91 (14.7%)**	-

Notes: F_{fmax}= maximum pullout force; F_{fu}= FRP strength force; $\tau_{max,av1}$= average bond stress at the bar-epoxy interface at F_{fmax}; $\tau_{max,av2}$= average bond stress at the glulam-epoxy interface at F_{fmax}; s_{fmax}= free end slip at F_{fmax}; s_{lmax}= loaded end slip at F_{fmax}; FAI – FRP/adhesive interfacial sliding; GAI – glulam/adhesive interfacial sliding; SPL – adhesive splitting; GS – glulam shear failure; CR – adhesive cracking; FF – FRP failure.

Table 5 – Main results obtained in the series GFRP1_D2

Specimen	F_{fmax} (kN)	F_{fmax} / F_{fu} (%)	$\tau_{max,av1}$ (MPa)	$\tau_{max,av2}$ (MPa)	s_{fmax} (mm)	s_{lmax} (mm)	*Failure mode*
GFRP2_D1_Lb30-1	14.78	23.95	15.69	10.65	0.371	0.258	FAI+CR
GFRP2_D1_Lb30-2	16.19	26.24	17.18	11.77	0.129	0.342	GAI
GFRP2_D1_Lb30	**15.49 (6.4%)**	**25.09 (6.4%)**	**16.44 (6.4%)**	**11.21 (7.0%)**	**0.25 (68.6%)**	**0.30 (19.7%)**	-
GFRP2_D1_Lb60-1	26.17	42.40	13.89	9.52	0.068	0.668	FAI+CR
GFRP2_D1_Lb60-2	22.81	36.95	12.10	8.27	0.066	0.413	FAI+GAI+CR
GFRP2_D1_Lb60-3	27.66	44.81	14.68	10.20	0.194	0.166	FAI+CR
GFRP2_D1_Lb60-4	22.74	36.85	12.07	8.36	0.066	0.222	GS+GAI
GFRP2_D1_Lb60	**24.85 (9.9%)**	**40.25 (9.9%)**	**13.18 (9.9%)**	**9.09 (10.3%)**	**0.10 (64.6%)**	**0.37 (61.7%)**	-
GFRP2_D1_Lb120-1	32.06	51.94	8.50	5.87	0.633	0.924	FAI+CR
GFRP2_D1_Lb120-2	35.32	57.21	9.37	6.26	0.133	0.884	GS+ FAI+CR
GFRP2_D1_Lb120	**33.69 (6.8%)**	**54.58 (6.8%)**	**8.94 (6.8%)**	**6.06 (4.6%)**	**0.38 (92.3%)**	**0.90 (3.1%)**	-

Notes: F_{fmax}= maximum pullout force; F_{fu}= FRP strength force; $\tau_{max,av1}$= average bond stress at the bar-epoxy interface at F_{fmax}; $\tau_{max,av2}$= average bond stress at the glulam-epoxy interface at F_{fmax}; s_{fmax}= free end slip at F_{fmax}; s_{lmax}= loaded end slip at F_{fmax}; FAI – interfacial failure FRP/adhesive; GAI – interfacial failure glulam/adhesive; SPL – adhesive splitting; GS – glulam shear failure; CR – adhesive cracking; FF – FRP failure.

Table 6 – Main results obtained in the series GFRP2_D1

Fig. 7 shows the principal failure modes obtained: (i) glulam shear failure (GS); (ii) glulam/adhesive interfacial sliding (GAI); (iii) FRP/adhesive interfacial sliding and adhesive splitting (FAI+SPL).

GS – Glulam shear failure

GAI – glulam/adhesive interfacial sliding

FAI+SPL – FRP/adhesive interfacial sliding + adhesive splitting

Figure 7 – Typical failure modes obtained

Fig. 8 presents the influence of the bond length (L_b) on the following parameters: pullout force efficiency (F_{max} / F_{fu}), loaded end slip (s_l), average bond strength at FRP/adhesive interface (τ_{av1}), and average bond strength at adhesive/glulam interface (τ_{av2}).

The F_{max} / F_{fu} ratio and the s_l have increased with the bond length. Larger L_b values need to be investigated to obtain the maximum values of for the F_{max} / F_{fu} ratio. The increase rate of s_l with L_b seems to increase with L_b, but up to L_b=120 mm the three series presented similar evolution. Fig. 8 also evidences the benefits in terms of F_{max} / F_{fu} and τ_{av1} when the rod is deeper installed into the groove. The better performance that can be achieved when selecting a bar of rougher surface is quite visible in terms of F_{max} / F_{fu} and bond stresses.

The decrease of the average bond stress with the increment of the bond length in all tested series seems to tend to an asymptotic value.

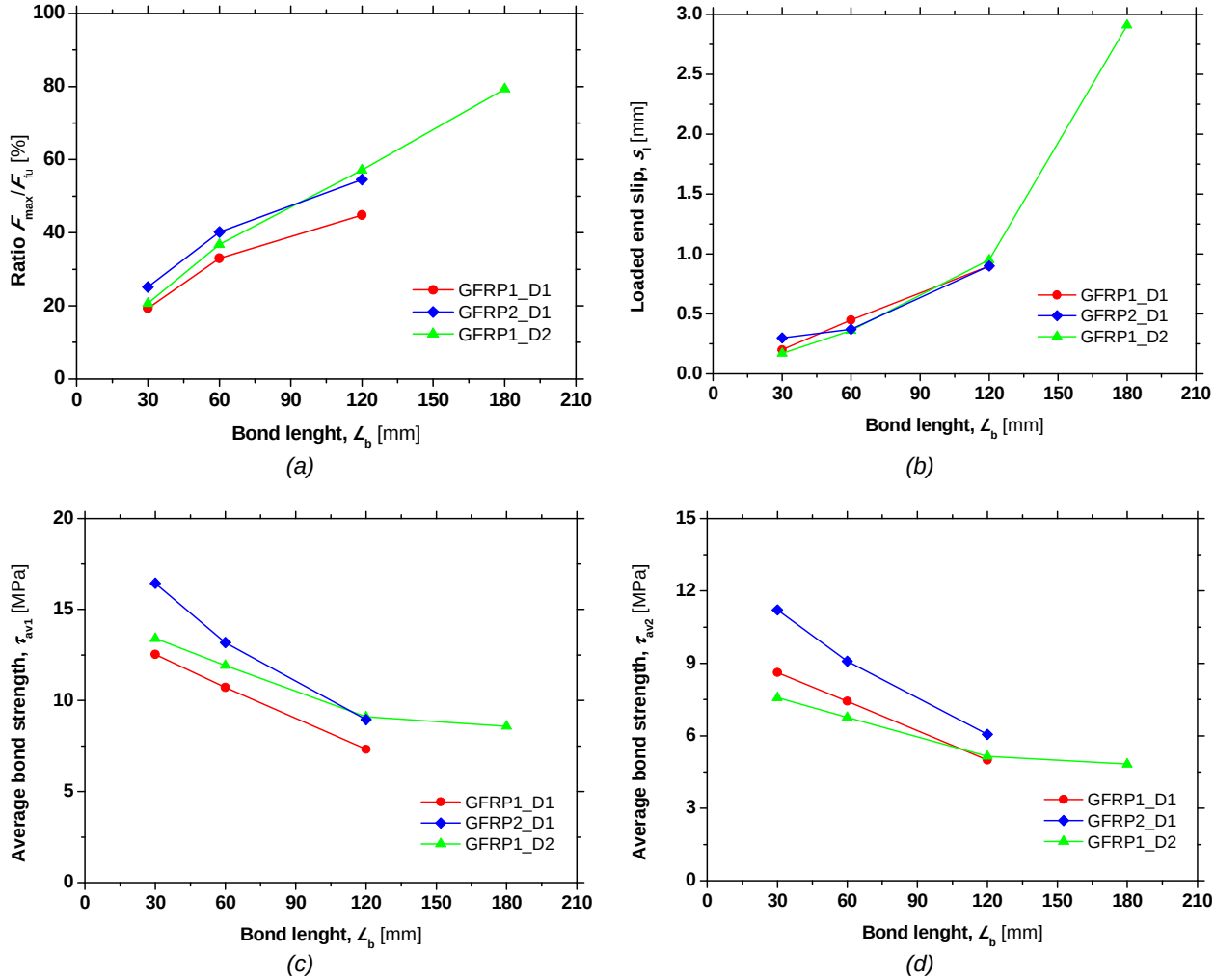

Figure 8 – Bond length influence on: (a) efficiency in terms of maximum load; (b) loaded end slip; (c) average bond strength τ_{av1}; (d) average bond strength τ_{av2}

Conclusions

The present work presented an experimental study on bond characterization between GFRP rods and glulam, using the near surface mounted strengthening technique, through pullout bending tests. The type of GFRP rod (GFRP1 and GFRP2), the groove geometry/FRP location (D1 and D2) and the bond length (L_b) were the main variables studied.

The pullout force, the loaded and free ends slips and the ratio between maximum pullout force and the FRP strength have increased with L_b, while the bond strength has decreased with the increase of L_b. A rougher surface has provided a better bond performance, as well as a deeper installation of the GFRP rod into the groove.

Failure modes included glulam shear failure, interfacial failure glulam/adhesive, interfacial failure FRP/adhesive and adhesive splitting.

Acknowledgements

This work is supported by FEDER funds through the Operational Programme for Competitiveness Factors - COMPETE and National Funds through FCT – Portuguese Foundation for Science and Technology under the project PTDC/ECM/74337/2006. The authors also like to thank all the companies that have been involved supporting and contributing for the development of this study, mainly: INEGI, S&P Clever Reinforcement, Portilame, MAPEI and Rothoblaas.

References

ACI 440.2R-08 (2008). “Guide for the Design and Construction of Externally Bonded FRP Systems for Strengthening Concrete Structures”, Reported by ACI Committee 440, American Concrete Institute, 80 pp.

Bank, L.C. (2004). “Mechanically-Fastened FRP (MF-FRP) – A Viable Alternative for Strengthening RC Members”, *Proceedings of CICE 2004*, Adelaide, Australia, 12 pp.

Barros, J.A.O.; Costa, I.G. (2010). “Bond Tests on Near Surface Reinforcement Strengthening for Concrete Structures”, *EN-CORE/fib Round Robin Testing Initiative*, Report 09.DEC/E-30 Department of Civil Engineering, University of Minho.

EN 408 (2003). “Timber structures - Structural timber and glued laminated timber. Determination of some physical and mechanical properties.” European Committee for Standardization (CEN), 31 pp.

ISO 527-2 (1993). “Plastics - Determination of tensile properties - Part 2: Test conditions for molding and extrusion plastics.” International Organization for Standardization (CEN).

ISO TC 71/SC 6 N Part 1 (2003). “Non-conventional reinforcement of concrete-test methods: Fiber reinforced polymer (FRP) bars.” International Organization for Standardization (CEN), 48 pp.

Jorge, M.A.P. (2010). “Experimental behavior of glulam-FRP systems.” MSc thesis, Department of Civil Engineering, University of Minho, 247 pp.

Sena-Cruz, J.M., Barros, J.A.O., Faria, R.M.C.M. (2001). “Assessing the embedded length of epoxy-bonded carbon laminates by pull-out bending tests.” International Conference Composites in Construction, 217-222.